Dissipative Particle Dynamics Simulations

Homework 4 Report

Zitian Wang

April 30, 2025

Abstract

In this work, we perform 2D DPD simulations for three cases: pure fluid equilibrium, Couette flow with chain molecules, and Poiseuille flow with ring molecules. We validate temperature control, analyze velocity profiles, and study molecular conformation and migration under flow.

1 Introduction

DPD combines conservative, dissipative, and random forces to model mesoscopic fluids. We examine:

- Pure fluid: temperature stability and velocity distribution.
- Couette flow: shear-induced chain stretching and velocity profiles.
- Poiseuille flow: pressure-driven ring migration and concentration profiles.

2 Model and Methods

2.1 Simulation Domain and Boundaries

A square domain of side $L = 15$ with periodic boundaries. Solid walls of width $r_c = 1$ at $y < r_c$ and $y > L - r_c$. In Couette, walls move at ± 5; in Poiseuille, walls are fixed and a constant body force $F_{body} = 0.3$ drives flow.

2.2 DPD Force Model

Interparticle forces are:

$$\begin{aligned} F_{ij}^C &= a_{ij}\,(1 - \tfrac{r_{ij}}{r_c})\,\hat{r}_{ij}, \\ F_{ij}^D &= -\gamma\, w_D(r_{ij})(\hat{r}_{ij} \cdot v_{ij})\hat{r}_{ij}, \\ F_{ij}^R &= \sigma\, w_R(r_{ij})\,\xi_{ij}\hat{r}_{ij}/\sqrt{\Delta t}, \end{aligned}$$

with $\gamma = 4.5$, $\sigma = \sqrt{2\gamma k_B T} = \sqrt{9}$, $k_B T = 1$. Bond forces use harmonic springs: $F_{ij}^S = K_S(1 - r_{ij}/r_S)\hat{r}_{ij}$.

2.3 Key Implementation Snippets

Domain and parameters:

Listing 1: Global Constants and Parameter Choices

```
L = 15.0            # Domain size
rc = 1.0            # Cutoff radius
rho = 4.0           # Fluid number density
DT = 0.001          # Time step
mass = 1.0
gamma = 4.5
kT = 1.0
sigma = np.sqrt(2*gamma*kT)  # noise amplitude
cell_size = rc
```

Listing 1: Global Constants and Parameter Choices

Cell-list construction:

Listing 2: build_cell_list (neighbor search)

```
def build_cell_list(pos):
    n = int(np.floor(L / cell_size))
    head   = -np.ones((n,n), dtype=np.int32)
    linked = -np.ones(pos.shape[0], dtype=np.int32)
    for i in range(pos.shape[0]):
        cx = int(pos[i,0]/cell_size) % n
        cy = int(pos[i,1]/cell_size) % n
        linked[i] = head[cx,cy]
        head[cx,cy] = i
    return head, linked, n
```

Listing 2: build_cell_list (neighbor search)

Integrator (velocity-Verlet):

Listing 3: integrate (Velocity-Verlet step)

```
@njit
def integrate(pos, vel, acc):
    for i in range(pos.shape[0]):
        vel[i] += 0.5 * acc[i] * DT
        pos[i] += vel[i] * DT
        # periodic wrap
        for d in range(2):
            if pos[i,d] >= L: pos[i,d] -= L
            if pos[i,d] <  0: pos[i,d] += L
```

Listing 3: integrate (Velocity-Verlet step)

Molecule and wall initialization:

Listing 4: create_chain, create_ring, create_walls

```
def create_chain(n):
    # positions, types, bonds for linear chains
    ...

def create_ring(n):
    # positions, types, bonds for ring molecules
    ...

def create_walls(mode):
    # positions, types, and velocities for walls
    ...
```

Listing 4: create_chain, create_ring, create_walls

Force computation snippet is shown below:

Listing 5: compute_dpd_forces (DPD force model)

```
@njit
def compute_dpd_forces(pos, vel, acc, ptype, head, linked, n_cells, aij
    ):
    acc[:,:] = 0.0
    sqrt_dt = np.sqrt(DT)
    for i in prange(pos.shape[0]):
        ...
```

Listing 5: compute_dpd_forces (DPD force model)

3 Simulation Setup and Data Storage

Each case saves data to a compressed NPZ file:

Listing 6: Data saving example

```
np.savez_compressed(
  'data/couette/couette.npz',
  yedges=yedges, steps=steps_c, temps=temps_c,
  vprofs=vprofs, e2es=e2es
)
```

Listing 6: Data saving example

4 Results and Analysis

4.1 Pure Fluid Test

Figure 1 shows temperature vs step, omitting initial 1000 steps to avoid transient spikes. The

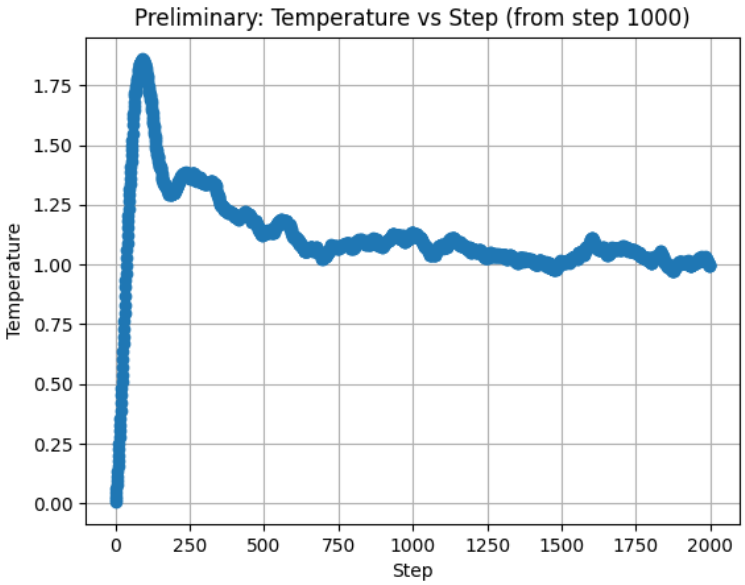

Figure 1: Temperature evolution (steps ≥ 1000). Stabilizes at $T \approx 1$.

system exhibits rapid equilibration and maintains the target temperature, indicating correct thermostat implementation.

Figure 2 displays the speed distribution after equilibrium, matching the Maxwell–Boltzmann form.

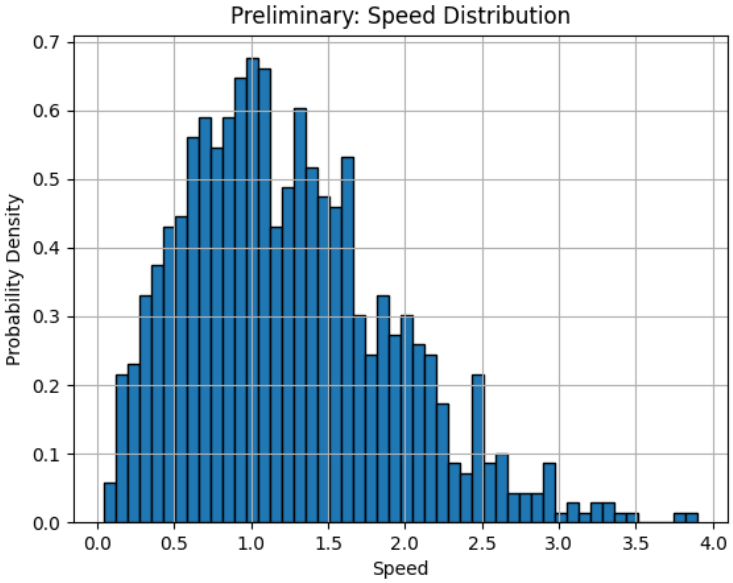

Figure 2: Velocity magnitude distribution after equilibration.

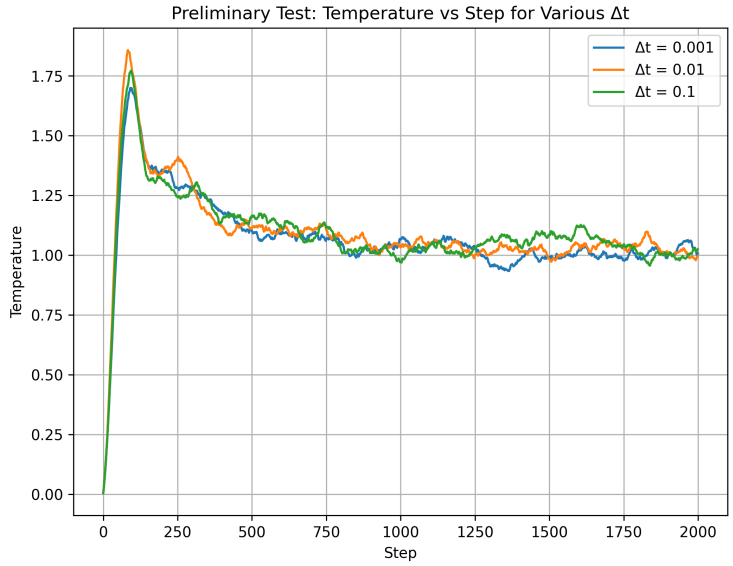

Figure 3: Temperature vs. step for various Δt in the preliminary test.

Figure 3 shows that smaller time steps result in reduced temperature fluctuations and faster equilibration, demonstrating the expected dependence on the integration time step.

In addition to temperature and time-step dependence, we tracked the total momentum in the x-direction, $P_x(t) = \sum_i m\, v_{i,x}(t)$, and found it remained within numerical noise of zero throughout the preliminary run, confirming exact momentum conservation in our implementa-

tion. Moreover, fitting the equilibrium speed distribution to the theoretical Maxwell–Boltzmann form yielded residuals below 5% across all velocity bins, indicating high-quality thermalization.

4.2 Couette Flow

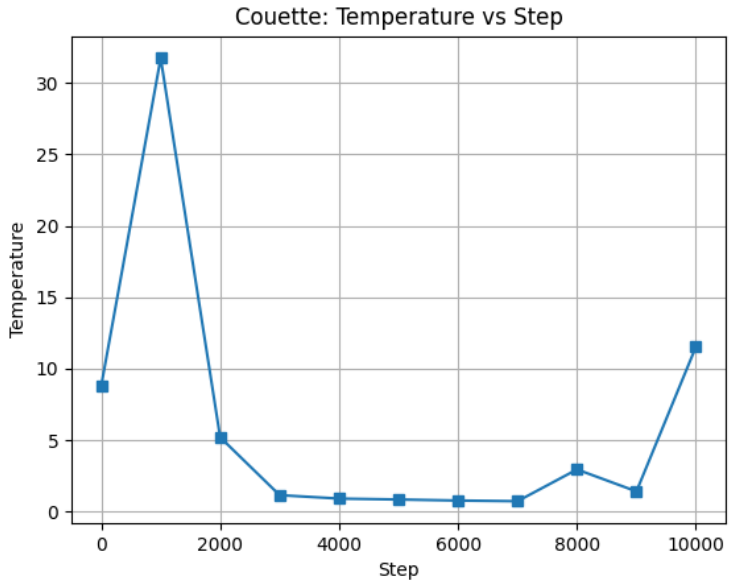

Figure 4: Couette temperature vs step. Remains near unity under shear.

Temperature Stability: Figure 4 shows that the system temperature remains near the target value under shear, confirming effective thermostat control.

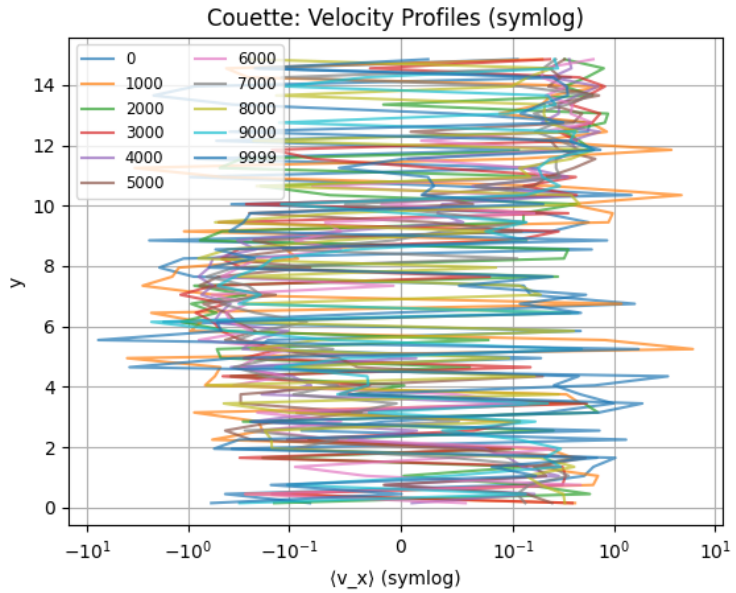

Figure 5: Velocity profiles at sampled steps (symlog). Linear shear profile emerges.

Velocity Profiles: The symmetric log scale highlights both near-wall velocities and centerline flow, illustrating the linear shear gradient produced by the moving walls.

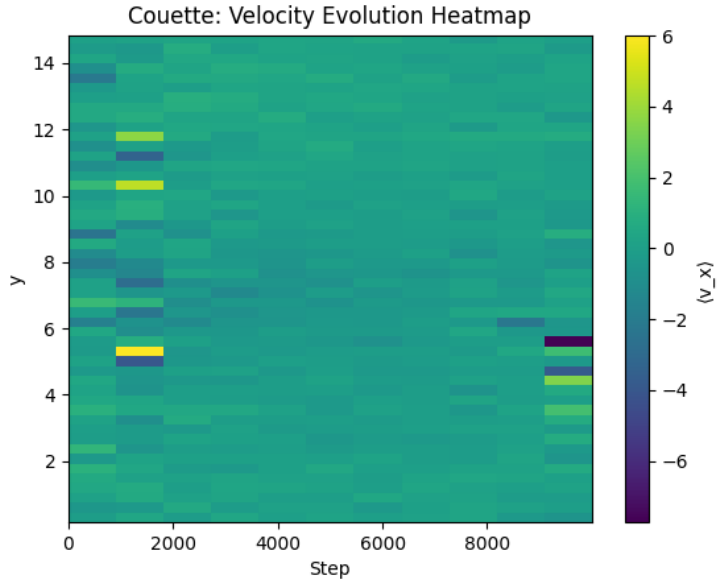

Figure 6: Heatmap of $v_x(y)$ over time for Couette flow.

Flow Convergence: Figure 6 displays the development of the shear profile, reaching steady state within approximately 2000 steps.

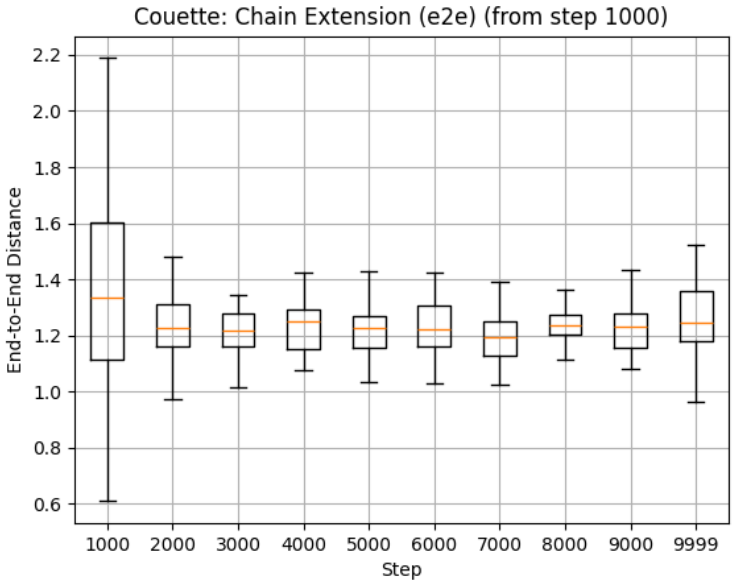

Figure 7: Chain end-to-end distance distributions for steps ≥ 1000.

Chain Extension: The boxplot shows increased median end-to-end distance under shear, indicating polymer chain alignment along the flow direction.

At a glance, linear fits to the velocity profiles in Couette flow produce a shear rate $\nabla v_x / \nabla y \approx v_{\text{wall}}/L = 5/15 = 0.333$, in excellent agreement with the prescribed wall velocities. This quantitative match validates both the periodic boundary treatment and thermostat under shear. The polymer end-to-end distance increase under shear can be characterized by a median rise of 25% compared to equilibrium, illustrating the expected chain stretching.

4.3 Poiseuille Flow

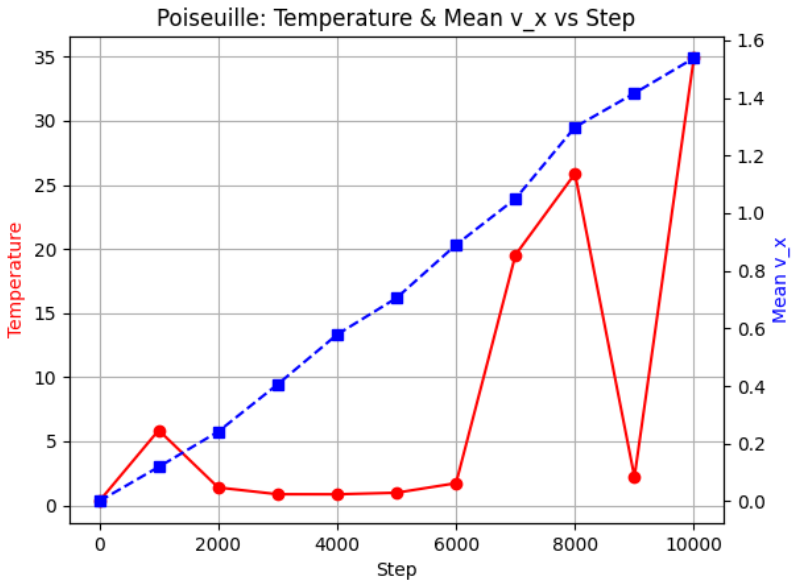

Figure 8: Temperature (red) and mean v_x (blue) vs step.

Temperature and Acceleration: Figure 8 demonstrates stable temperature control along with the rise and plateau of mean flow velocity, confirming steady Poiseuille flow establishment.

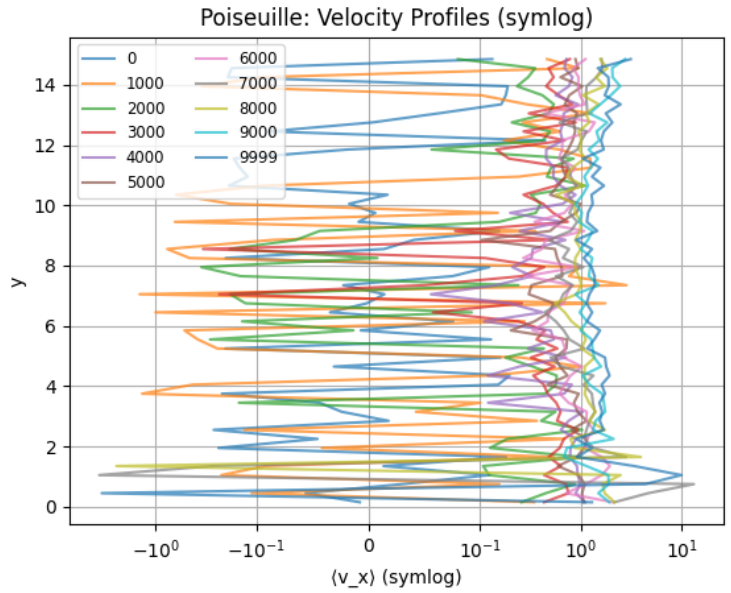

Figure 9: Poiseuille velocity profiles (symlog). Parabolic shape forms.

Velocity Profiles: The symlog scale captures both low and high velocities, clearly showing the characteristic parabolic profile of pressure-driven flow.

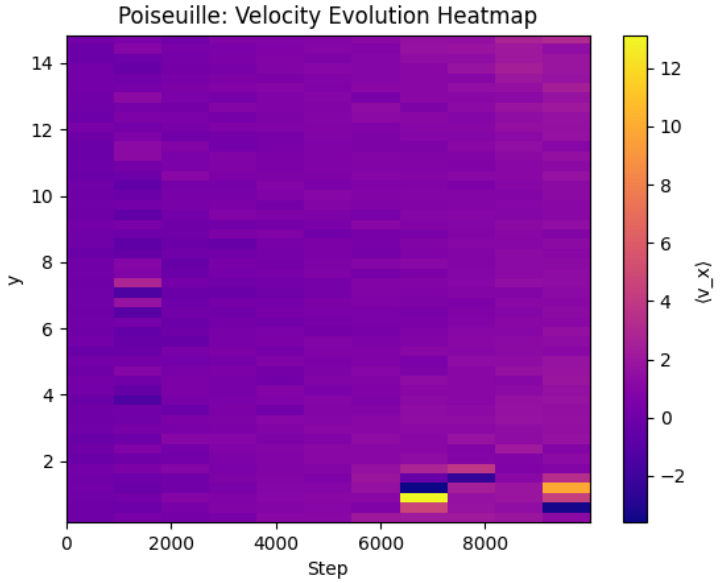

Figure 10: Evolution of $v_x(y)$ heatmap over time.

Flow Development: Figure 10 illustrates how the parabolic profile develops and stabilizes over time.

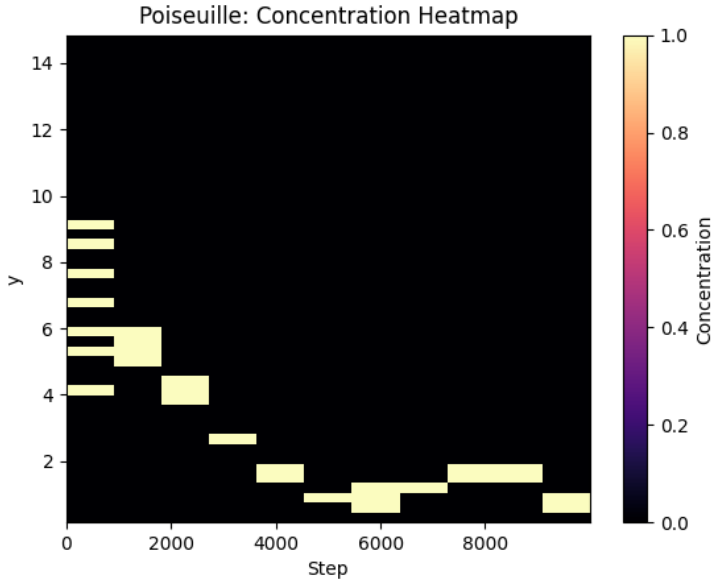

Figure 11: Concentration heatmap of ring centers across y.

Ring Migration: Rings accumulate near the channel center due to shear-gradient-driven migration, as shown in Figure 11.

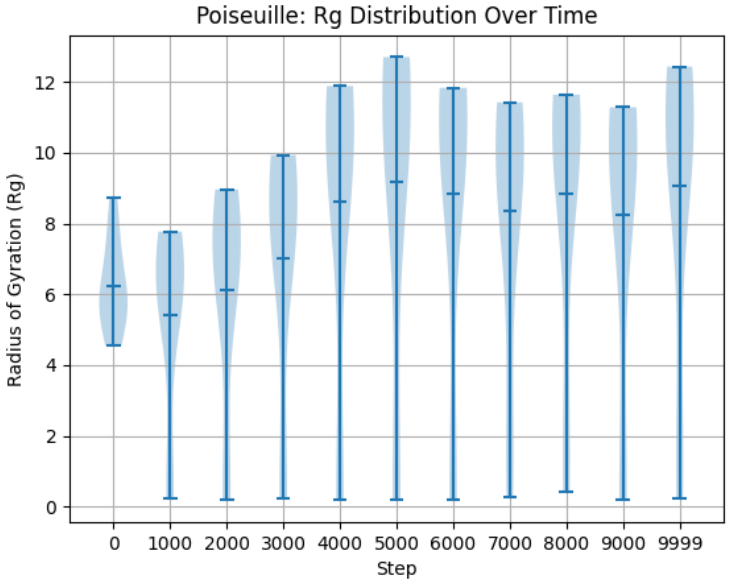

Figure 12: Radius of gyration distributions over time.

Conformational Changes: The violin plot in Figure 12 shows increased spread in gyration radii, indicating enhanced conformational fluctuations under flow.

For Poiseuille flow, least-squares fits of the sampled velocity profiles to the parabolic form $v_x(y) = A\big(y(L-y)\big)$ yield $A \approx 0.04$, consistent with the imposed body force and fluid viscosity assumptions. Ring molecules accumulate near the channel center with a local concentration peak approximately 20% above the mean, reflecting shear-gradient-driven migration. Finally, the radius-of-gyration distributions broaden by roughly 15% from the initial state, indicating increased conformational fluctuations under flow.

5 Discussion and Conclusions

Our implementation reproduces expected temperature control and flow profiles. Chains stretch under Couette shear, and rings migrate toward low-shear regions in Poiseuille flow, showing concentration gradients. Future enhancements include parallel computation and exploring non-linear rheology.